

ARTICLE

Design and Effectiveness of Coastal Protection Structures: Case Studies and Modelling Approaches

Leo C. van Rijn 

LVRIS-Consultancy, Domineeswal 6, Blokzijl 8356DS, The Netherlands

ABSTRACT

Beach groynes are structures for erosion protection along sandy coasts near inlets and can reduce the coastal erosion substantially, but open groynes cannot stop erosion completely because sand can be removed from the groyne compartments by cross-shore processes. Beach groynes should be designed with sufficient bypassing of sand to minimise erosion. Regular beach maintenance is required to keep a sufficient beach width for recreational purposes. The effectiveness of groyne compartments can be significantly improved by using T-head groynes or by using a submerged sill or breakwater in between the groynes. An economic evaluation shows that the beach maintenance costs over 50 years may be substantially higher than the construction costs of a submerged breakwater. An important parameter to be studied is the longshore transport, which requires detailed information of the wave climate, preferably based on measured data (offshore buoys) in combination with deep water wave modelling. Various models have been used to determine the net longshore sand transport and coastline changes. The design of groynes to reduce coastal erosion is illustrated by three field cases (Atlantic coast near Soulac, France; Lagos coast, Nigeria and Black Sea coast, Romania). These example cases show that beach groynes are effective structures, but sufficient bypassing of longshore sand transport is essential to minimise erosion. Regular beach fills in the groyne compartments may be required at high-energy (exposed) coasts. A submerged or emerged breakwater can be built between the groynes to protect the beach in the groyne compartments against erosion by cross-shore processes.

Keywords: Coastal Protection Structures; Coastal Recession; Coastal Erosion Modelling

*CORRESPONDING AUTHOR:

Leo C. van Rijn, LVRIS-Consultancy, Domineeswal 6, Blokzijl 8356DS, The Netherlands; Email: info@leovanrijn-sediment.com

ARTICLE INFO

Received: 3 February 2025 | Revised: 4 March 2025 | Accepted: 20 March 2025 | Published Online: 22 April 2025
DOI: <https://doi.org/10.30564/jees.v7i5.8649>

CITATION

van Rijn, L.C., 2025. Design and Effectiveness of Coastal Protection Structures: Case Studies and Modelling Approaches. Journal of Environmental & Earth Sciences. 7(5): 72–95. DOI: <https://doi.org/10.30564/jees.v7i5.8649>

COPYRIGHT

Copyright © 2025 by the author(s). Published by Bilingual Publishing Group. This is an open access article under the Creative Commons Attribution-NonCommercial 4.0 International (CC BY-NC 4.0) License (<https://creativecommons.org/licenses/by-nc/4.0/>).

1. Introduction

Chronic erosion is a problem at many beaches, particularly near tidal inlets^[1–3]. Basically, two options are available: 1) do nothing and accept erosion; 2) hold the line by regular (soft) beach nourishments or by the construction of hard permanent structures.

Generally, coastal structures such as groynes, breakwaters, and revetments are built to significantly reduce coastal beach erosion and maintain a minimum beach width for recreation; see reviews^[1, 3–9]. Hard structures such as groynes and breakwaters are, however, no remedy for dune and soft cliff erosion during storm conditions with relatively high surge levels (1 to 3 m above mean sea level (MSL)). Revetments with mild slopes (1 to 3 or milder) up to at least 5 m above MSL have to be built to stop dune and cliff erosion completely. Usually, these latter structures are built in regions (along boulevards of beach resorts) where natural dunes are absent or have been removed for recreational purposes.

A modern development along the coasts of major beach cities is the replacement of small-scale, groyne compartments by wide pocket-type beaches consisting of one or two long terminal groynes and submerged detached breakwaters parallel to the shore creating a relatively long uninterrupted and visually attractive beach^[10]. Submerged breakwaters do not suffer from the adverse aesthetic impacts of groynes and emerged breakwaters.

Instructive examples of these types of ‘harnessed’ solutions with many structures are the Mediterranean coast of Sitges, at about 20 km south of Barcelona, and the black sea coast south of Constanta in Romania. Although these solutions are most effective in reducing the storm-induced beach erosion, they may not be the most cost-effective solution. It should always be studied whether the relatively expensive detached breakwater between the tip of the groynes can be omitted. The coastal cell between the groynes will then be open for wave attack, requiring more beach maintenance (beach fills), but this may be cheaper in the long term.

Basic research questions of coastal protection measures are: 1) what is the most effective method for coastal protection (minimum erosion, maximum accretion); 2) what is the best method to minimise the downdrift erosion of hard structures and 3) How can simple longshore and cross-shore coastal models be used to predict the short-term and long-term morphological consequences of coastal protec-

tion structures. Ideally, the complicated hydrodynamic and morphodynamic processes in the nearshore coastal zone can only be represented in a 3D model. At the present stage of research, a reliable and accurate 3D model is not available. Two-dimensional horizontal models based on depth-averaged parameters are in development, but these models are not sufficiently accurate and require excessive runtimes for large domains and long-term predictions. Therefore, it is often necessary to apply separate models for the longshore and cross-shore directions and integrate the results of these models in a pragmatic engineering way. The novel aspect of the present paper is the application, calibration and integration of these types of models for practical projects. Thus, the novelty lies in the applied use of existing models for three practical cases, not in model improvement. Herein, three complicated coastal projects including all relevant field data are studied and discussed. The basic physical processes, the design requirements and the characteristics of hard structures are discussed in Section 2. The models and modelling approaches used for the design of effective hard structures and the erosion involved are presented in Section 3. Three practical coastal projects, including beach groyne design in France (Aquitain coast), in Nigeria (Lagos coast) and in Romania (Black Sea coast), are presented and discussed in Sections 4, 5, and 6 to learn lessons for coastal engineers. Finally, many practical guidelines for model application and schematisation are presented and discussed in Section 7.

2. Design Requirements and Characteristics of Hard Structures

2.1. General

This section summarises the basic coastal processes and the design requirement for adequate coastal protection against erosion (Section 2.2), followed by an overview of the characteristics of the most promising coastal protection structures (groynes, breakwaters and revetments; Section 2.3).

Coastal erosion is strongly related to the variability of cross-shore and longshore sand transport (LST) processes. When the incoming waves are normal to the coast, wave shoaling and wave breaking occur in the nearshore zone (surf zone). Breaking waves normal to the coast generate a net seaward-directed current (known as undertow; 0.1 to

0.5 m/s) in the lower part of the water column, which carries suspended sediments away from the beach to deeper water (beach erosion due to cross-shore transport). When the incoming waves are oblique (under an angle) to the coast, the breaking waves generate a longshore current (range of 0.3 to 1.5 m/s) which carries sediments along the shore (longshore transport).

2.2. Design Requirements

The most important design requirements for effective coastal structures along sandy beaches are:

- protection against erosion by currents and waves; the erosion of the beach and dune face should be minimal during storm events (beach-dune revetments may be required in extreme cases);
- smooth wave energy dissipation (sloping surfaces rather than vertical walls);
- sufficient beach width for recreation; the beach width in the summer season should be about 50 m (minimum); beach width can be increased by placing beach fills, if sand is abundantly available;
- minimum downdrift erosion; the LST should not be completely blocked by the structure; sufficient bypassing should be promoted (relatively short and low structures);
- easy to build; submerged structures should be designed in a way that they can be built from the landward side;
- aesthetic appearance in harmony with nature; building materials should be rock rather than concrete and steel and placed in an orderly way (no riprap or rubble mound above water).

2.3. Coastal Structures

Given the aforementioned design requirements, the most promising coastal protection structures are groynes, submerged breakwaters, and revetments. **Table 1** presents a summary of requirements.

Groynes

Straight groynes are long, narrow structures perpendicular or slightly oblique to the shoreline extending into the surf zone and are massively used all over the world, because they are easy and relatively cheap to build. High-crested

groyne-type structures are mostly used at severely erosive beaches with recession rates > 2 m/year (near inlets) and sufficient supply of sand from updrift. The main function of these groynes is to reduce the longshore tide and wave-driven currents and associated sand transport rates. Groynes can also be used to protect beach nourishments and to widen local beaches at sheltered sites. Two types of groynes can be distinguished: a) impermeable, high-crested structures: crest levels above +1 m above MSL and b) permeable, low-crested structures (wooden piles): crest level between mean low water (MLW) and mean high water (MHW).

The length of the groynes (L) should be smaller than the width of the surf zone during storm conditions to promote sufficient bypassing of sand. Groyne spacing (S) should be in the range of $S = 1.5$ to $3L$; groyne tapering can also be used (reduced lengths at downcoast end of groyne field). Groyne crest levels should not be much larger than about +1 m to allow bypassing of sediment during high tide and stormy conditions to reduce lee-side erosion. High crest levels prevent sediment from bypassing and are unattractive for beach recreation.

Along beaches of fine sand at exposed sites, groynes will only reduce beach erosion, but the erosion cannot be stopped completely, as the waves can easily propagate into the compartments, causing erosion due to cross-shore processes, particularly in the case of relatively steep beach slopes. The trapping of sand inside the groyne compartments is not very high and mostly absent due to the generation of water level (setup) differences, circulation flows and rip currents^[11]. These findings are confirmed by numerical modelling^[12]. The trapping of sand increases with decreasing spacing (narrow cells are more effective than wide cells).

The effectiveness of straight groynes can be substantially increased by using T- or L- head groynes to increase the trapping of sand and to prevent/diminish the generation of rip currents near the groyne heads (**Figure 1**). The length of the head should be of the same order of magnitude as the length of the groyne ($L_{\text{head}} \cong L$).

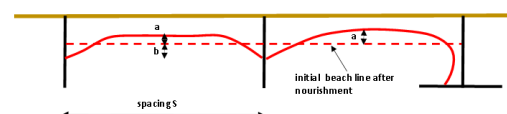


Figure 1. Beach changes within groyne compartments due to long-shore transport processes ($a \cong 0.02\text{--}0.04 S$ for straight groynes; $a \cong 0.04\text{--}0.06 S$ for T-head groynes).

Table 1. Summary of requirements.

Type of Structure	Summary of Requirements
Groynes	<ol style="list-style-type: none"> 1. Most effective at beaches with recession rates > 2 m/year (near inlets) 2. Length of the groynes (L) should be smaller than the width of the surf zone during storm conditions. 3. Groyne spacing (S) should be in the range of $S = 1.5$ to $3L$. 4. Groyne tapering with reduced lengths at downcoast end should be used. 5. Groyne crest levels should not be much larger than about +1 m at the tip for sufficient bypassing of sand during high tide and stormy conditions. 6. Groynes should be built up to the dune foot in macro-tidal conditions. 7. Trapping of sand in groyne cells can be increased by using T- or L- head groynes.
Submerged and emerged breakwaters	<ol style="list-style-type: none"> 1. Emerged breakwaters are more effective than submerged breakwaters, but are less attractive from an aesthetic point of view. 2. The crest of submerged breakwaters should be sufficiently wide (about 20 m) for wave breaking on the structure (not behind the structure). 3. The crest of submerged breakwaters should be very close to the mean sea level (0.5 to 1 m below MSL). 4. Submerged breakwaters are most effective at sites with micro tidal range (< 0.5 m)
Revetments	<ol style="list-style-type: none"> 1. Slope of the revetment should be as mild as possible (not steeper than a slope of 1 to 3). 2. The structure should have effective toe protection. 3. The crest of the revetment should be well above the highest storm surge level resulting in a crest level at +5 m above mean sea level along open coasts and up to +7 m at locations with extreme surge levels. 4. Short groynes can be built at the toe of the revetment to deflect strong longshore current creating scour at the toe of the structure.

Erosion between the groynes can only be mitigated by regular beach fills to stabilise the beach or by the construction of a submerged breakwater between the groynes. Nowadays, the design of groyne fields along exposed, eroding coasts with recession rates exceeding 2 m/year is nearly always combined with the (regular) placement of beach fills inside the groyne compartments to widen the beaches [2, 3, 13–15].

The beach shape inside a compartment with T-head groynes primarily depends on the trapping of sand and the circulation flows and wave patterns generated inside the compartment. When the updrift longshore transport rate is high and/or the groyne length is relatively short, sand by passing will occur and the compartment may be gradually be filled

by trapped sand, as shown by DELFT3D-simulations for one groyne cell (length = 400 m; spacing = 500 m) in **Figure 2**. The DELFT3D-model is a sophisticated model which computes currents, waves and LST at every grid point and also the corresponding erosion and accretion of sand in and around the groyne cell on short time scales (months). The model is too detailed for long-term simulations. It can be seen in **Figure 2** that the most right groyne blocks the LST resulting in coastal accretion. Sand can enter the groyne compartment through exchange currents. LST is gradually restored on the left side of the groyne compartment resulting in coastal erosion (**Figure 2**).

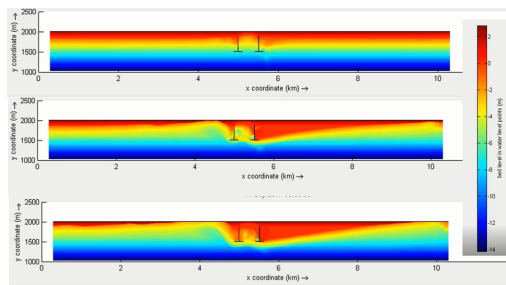


Figure 2. Morphological patterns at 2 time moments (LST from right to left) near T-head groynes based on DELFT3D-runs.

Submerged shore-parallel breakwater

A submerged (reef-type) breakwater is herein defined as a long, shore-parallel structure with a relatively high crest level (0.5 to 1 m below MSL) protecting a section of the shoreline by forming a filter to the waves (dissipation of incident wave energy due to breaking). The crest should be sufficiently wide (about 20 m) for wave breaking on the structure (not behind the structure). Submerged breakwaters are attractive as they are not visible from the beach. Submerged structures cannot stop beach and dune erosion completely during storm conditions, as the lower waves will pass over structure to attack the dune or cliff front. Supplementary beach nourishments may be required to deal with local storm-induced shoreline erosion. Revetments can be built at the upper beach and dune front to stop erosion completely (at beach boulevard sites). Downdrift erosion is generally manageable as longshore transport is not completely blocked by low-crested structures.

El-Sharnouby and Soliman have evaluated the behaviour of various shore protection structures (groynes, revetments, breakwaters) along the micro-tidal coast of Alexandria in Egypt, which is a sand starvation coast due to the blocking of sand transport in the Nile River (reservoirs)^[9]. They found that the performance of a long, massive submerged breakwater with a high crest level (0.7 m below MSL; 1.7 m below water level during extreme storms due to an extra surge of 1 m) parallel to the shore at about 200 to 300 m from the beach was rather good. The crest was wide (30 m) to ensure sufficient wave breaking on the crest and not behind the crest. Overlapping gaps were built on both sides of the breakwater. Water flushing in the lee area was measured to be of the order of 5 days. Waves were smaller than 0.5 m during 90% of the time. The beach in the lee of the breakwater was rather stable over the period 2009 to 2024 after completion of the structure (2006 to 2009). Some initial

beach erosion due to planform adjustment was observed after a major storm in 2010^[16].

The best performance of submerged breakwaters can be expected in micro-tidal conditions with tidal range < 1 m (Mediterranean, Baltic Sea, Black Sea), because the water depth above the crest can be designed to be small (order of 1 m). Submerged breakwaters are not effective in macro-tidal conditions with a tidal range of 3 to 5 m, because the water depth above the crest will vary too much and high waves can pass over the structure during flood/storm conditions. Disadvantages of detached submerged breakwaters are the relatively high construction and maintenance costs, inconvenience/danger to swimmers and small boats.

Revetments

Revetments are shore-parallel armoured structures to protect the beach and dune face against episodic storm-induced erosion and/or long-term chronic erosion. Generally, these sloping structures are built along a limited section of the shoreline as a last defence line against the waves, when natural beaches and dunes are too small or too low to prevent erosion due to high waves. It is the “end of the line” solution, if no other solution helps to solve the problem of erosion and/or flooding (high surge levels). A revetment is an armour protection layer (consisting of light to heavy armour blocks on a filter layer) on a mild slope. To reduce scour by wave action and wave reflection at the toe of the structure, the slope of the revetment should be as mild as possible (not steeper than 1 to 3) and the structure should have effective toe protection. The crest of the revetment should be well above the highest storm surge level resulting in a crest level at +5 m above MSL along open coasts and up to +7 m at locations with extreme surge levels.

Revetments are very effective in complete prevention of local shoreline erosion (dunes and soft cliffs), but these types of structures cannot change the basic cause of the erosion processes. Hence, erosion of the seabed at the toe of the structure will generally continue which may easily lead to deep scour holes and undermining of the structure (requiring deep foundation level and/or toe protection). Downtide erosion will usually occur at locations where no structures are present. Continuing shoreface erosion may ultimately lead to an increased wave attack intensifying the transport capacity and hence intensified erosion (negative feed-back system). Short groynes are often constructed to reduce scour

at the toe of the revetment by deflecting nearshore currents. Seabed protection may be necessary in case of strong tidal currents passing the structure (sea dike protruding into sea).

3. Models and Methodology

3.1. General

An important side effect of coastal protection structures is the downdrift erosion by sand transport processes, which is explained in Section 3.3. Practical (existing) engineering models for the computation of the wave and sand transport parameters and bed level changes in longshore and in cross-shore direction are briefly described in Sections 3.2 and 3.3.

3.2. Models

The best overall approach to model coastal morphology is the application of complex wave and (tidal) flow models (for example, DELFT3D model package including the SWAN wave-model). These types of models compute the tide-, wind- and wave-driven currents, the wave heights and directions and the sand transport rates due to currents and waves in each grid point and at each time step. The bed level changes (bathymetry) are computed from the spatial gradients of the sand transport rates. In the case of a large-scale spatial domain (50 km), this often is a major modelling effort (work of months) which is most appropriate for the design phase of a project. It is noted that these sophisticated models can only be used for short-term computations (up to 1 year) at present computer power.

In the exploring feasibility phase of a project, it may be more appropriate to apply a more simple and pragmatic approach with separate models for the longshore and the cross-shore direction (quick scan approach). The models used in this paper are the LONGMOR-model for the longshore direction and the CROSMOR-model for the cross-shore direction. Both models can be set up and run quickly (1 day). The LONGMOR-model is a 1D numerical coastline model (FORTRAN-code) which computes the wave height and wave incidence angle at the breaker line, the LST rate in the breaker zone based on semi-empirical equations and the corresponding coastline changes over time due to alongshore gradients of the sand transport rate in the breaker zone^[17, 18].

A 1D LONGMOR-model run can be set up in 1 hour and has a run time of 15 minutes for a coastline of 30 km over 30 years.

The CROSMOR-model is a 1D numerical (Fortran) model which computes wave propagation (wave height and direction), tide and wave-driven longshore currents, cross-shore and LST and cross-shore bed level changes along one single bed profile (cross-section) normal to the coast on time scales up to 5 years^[19–21]. The propagation and transformation of individual waves (wave by wave approach) along the cross-shore profile is based on numerical solution of the wave energy equation for each individual waves including the effects of shoaling, refraction, bed friction, wave asymmetry^[22] and wave breaking. Wave-induced set-up and set-down and breaking-associated longshore currents are also modelled. The velocity due to low-frequency waves in the swash zone is also taken into account by an empirical method. The depth-averaged return current under the wave trough of each individual wave (summation over wave classes) is derived from linear mass transport and the water depth under the wave trough. The transport of sand and gravel is based on the sand transport formulations of van Rijn^[23–26]. The sediment transport rate is determined for each wave (or wave class), based on the computed wave height, depth-averaged cross-shore and longshore velocities, orbital velocities, friction factors and sediment parameters. A CROSMOR-model run can be set up in 1 hour and has a run time of about 30 minutes for simulation of a cross-shore bed profile (length of 3 km) over 1 year.

Another pragmatic model is the DIFSAND-spreadsheet model, which is a supporting model for computation of the wave height and the wave angle and associated LST at the breaker line inside the wave diffraction zone (in lee of breakwaters or inside beach compartments; wave diffraction is explained in Section 3.3). The results of this model can be used for finetuning of the LST related to wave diffraction in the LONGMOR-model.

3.3. Modelling Approach for Downdrift Erosion

The physical processes of downdrift erosion in the lee of a long groyne or breakwater are explained and discussed from a practical engineering point of view, as reliable and accurate 2D/3D morpho-dynamic models (flow and wave models) are not yet available to compute the complicated

longshore and cross-shore transport processes in the lee of these types of structures.

A long structure normal to the shore interrupts part or all of the LST resulting in accretion on the updrift side and erosion on the downdrift side (east side in **Figures 3** and **4**). In the lee zone where wave diffraction processes occur, the wave-driven longshore current and sand transport is gradually growing to new equilibrium values (see example DELFT2D-model in **Figure 3**). Similar processes do occur inside the compartments of a groyne field. To address this problem, it is necessary to schematize the wave diffraction processes so that the wave heights in the diffraction zone and associated sand transport rates can be computed.

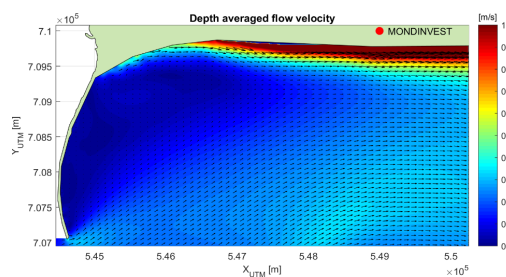


Figure 3. Wave-driven flow velocities in lee of long groyne; waves ($H_{s,0} = 4$ m) from South-West.

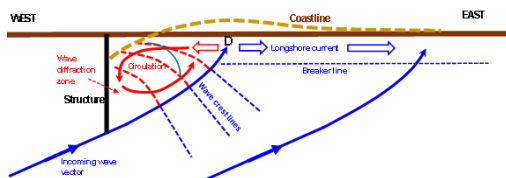


Figure 4. Diffracted waves and circulation currents in lee of structure (D = divergence point).

Wave diffraction is the process by which energy spreads laterally to the dominant direction of wave propagation^[27–30]. In this way, wave energy can enter the lee zone of the breakwater structure^[27], as shown in the wave diffraction zone (red zone) in **Figure 4**. Breaking waves in the lee zone of the structure are lower (with lower wave setup) than the breaking waves further away from the structure. This generates a longshore current towards the structure (red arrow, **Figure 4**) which is opposite to the longshore current further away to the east. The longshore current towards the structure is part of the circulation flow generated in the lee zone. At point D (**Figure 4**), there is a divergence zone where the longshore current is about zero and coastal erosion is maximum. The diffracted wave heights in the lee zone of the breakwater are

significantly smaller than the incoming waves at the tip of the breakwater ($H_s = K_d H_{s,I}$ with $K_D < 1$)^[27–30]. The angles of the waves inside the diffraction zone are quite small (waves are almost perpendicular to the shoreline). Outside the diffraction zone (on the east side of point D), the wave-induced longshore current will gradually increase to its full strength further away from the diffraction zone. Existing wave models (SWAN-model) are not very good in wave predictions inside diffraction zones^[31].

Wave diffraction and associated LST can be computed by the DIFSAND-model, which is based on the engineering method of Kamphuis for irregular waves with a broadband directional spectrum^[32]. The K_d -coefficients are parameterised for the full range of wave direction conditions. The angle of the diffracted waves at the breaker line in the lee of the structure is approximated by: $\theta_{br,d} = (K_d)^{0.38} \theta_{br}$ with $\theta_{br,d}$ = angle of diffracted wave ray (to shore normal) at the breaker line in the diffraction zone; θ_{br} = angle of wave ray at the breaker line without structure. The LST can be computed by the DIFSAND-model when the wave height and wave angle at the breaker line in the wave diffraction are known.

3.4. Example Cases

Three practical example cases related to the modelling of accretion and erosion around hard structures are explained hereafter in Sections 4, 5 and 6, being:

- modelling of coastline changes around short groyne for beach stabilisation, Soulac, France (Section 4);
- modelling of coastline changes around long harbour breakwater; Lagos, Nigeria (Section 5);
- modelling of erosion in groyne compartments and the effect of submerged breakwaters, Black Sea coast, Romania (Section 6).

It is emphasised that the focus is on the application of existing models (not new theory or new equations). Available field data are used for calibration of the models. Based on this, practical guidelines for model application and schematisation are given at the end of each section.

4. Example Case: Modelling of Short Groyne for Beach Stabilisation, Soulac, France

4.1. General

This example case refers to the design of a short, single groyne in 2014 (Barriquand groyne, north of Soulac, see **Figure 5**) along the Atlantic Ocean coast of France, with the aim of increasing the local beach width updrift of the groyne and minimising downdrift erosion by providing sufficient bypassing of sand.

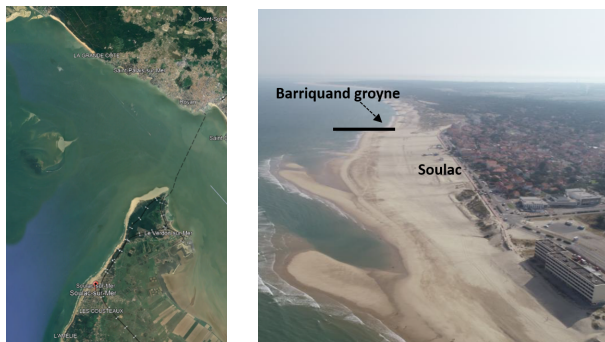


Figure 5. Inlet Garonne France and location of Barriquand groyne near Soulac (constructed in 2014).

4.2. Site Description

The sandy Aquitaine coast west of Bordeaux in France extends from the Gironde Estuary at the north to the Adour River at the south (**Figure 5**). It is an almost continuous 230 km long open beach-dune system. The longshore drift is generally northward close to the Gironde inlet. Annual residual flux volumes are between 200,000 and 400,000 m³/y in the Gironde area^[33]. Measured coastline erosion is between 15 m³/m/yr and 20 m³/m/yr^[34, 35]. Casagec reports values of 5 to 10 m/year between Négade and Le Signal (distance of about 4500 m from inlet)^[36].

4.3. Environmental Conditions

The local tidal data (Point La Grave) are: HAT = 5.9 m CD (Highest Astronomical Tide); MHWS = 5.3 m CD; MHWN = 4.35 m CD; MSL = 3.29 m CD; MLWN = 2.1 m CD; MLWS = 1.1 m CD and LAT = 0.54 m CD (Lowest Astronomical Tide). The tidal ranges are: 2.25 m neap; 3.22 m mean and 4.2 m spring. Surge levels are up to 1.2 m once per 100 years. The peak flood and ebb current velocities at a depth of 3 to 5 m are: 1 to 1.5 m/s near the inlet, 0.4 to 0.6 m/s near Barriquand groyne and 0.2 to 0.4 m/s further south. About 90% of the wave energy is in the sector 270° ± 15°. Extreme offshore wave heights are: $H_{s,1 \text{ year}} = 7.4 \text{ m}$;

$H_{s,10 \text{ years}} = 9.3 \text{ m}$ and $H_{s,100 \text{ years}} = 10.3 \text{ m}$.

Based on analysis of beach sand samples, the average beach sand diameter between Point La Grave near the inlet and Point La Négade varies in the range of 0.27 to 0.71 mm with an average value of $d_{50} \cong 0.39 \text{ mm}$.

Typical beach profiles between the Gironde inlet and Négade (13 km from the inlet) are given in **Figure 6**.

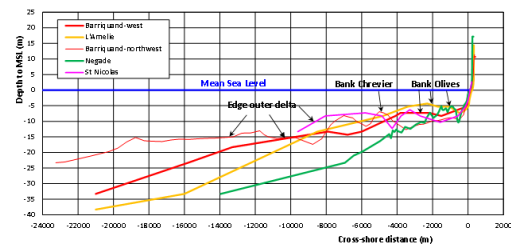


Figure 6. Cross-shore profiles to deep water between St Nicolas (Close to inlet) and Négade (13 km from inlet).

Most profiles of **Figure 6** cross the outer delta. The beach slope above MSL is about 1 to 40, the slope of the nearshore zone with depth to -5 m (below MSL) is about 1 to 60. The beach width between Low Water (LW) and dune foot is in the range of 150 to 200 m. The width of the dry beach is rather small, with values of 50 m at St Nicolas and Barriquand and almost nil (<10 m) at L'Amélie and Négade. The High Water (HW) line is close to the dune foot at these latter two locations indicating erosive beach conditions.

Figure 7 shows 2 profiles south of the Barriquand groyne (see **Figure 5**) in October 2015 and 2019. Both profiles show substantial accretion (about 200 m³/m in Profile 1.87 and 130 m³/m in Profile 2.54 over 4 years) which is most likely caused by the extension of the Barriquand groyne in summer 2014 blocking part of the north-going LST. Assuming a longshore-averaged accretion of 160 m³/m over a distance of about 1 km between Le Signal and Barriquand groyne, the total deposition volume is 1000x160 = 160,000 m³ over four years as positive effect of the groyne extension in 2014 which is equivalent to 40,000 m³/year. In the period 2014–2018, about 60,000 m³ of sand has been removed (excavated) from the region south of the Barriquand and placed by trucks in the region of Le Signal (shift from downdrift to updrift). In total, about 200,000 m³ of sand has been replaced between 2018 and 2021. The deposition volume north of Le Signal is estimated to be about 300,000 m³ over six years (2014–2020) or 50,000 m³/year. The net erosion between Camping LS and le Signal is estimated to be about 30,000 m³/year.

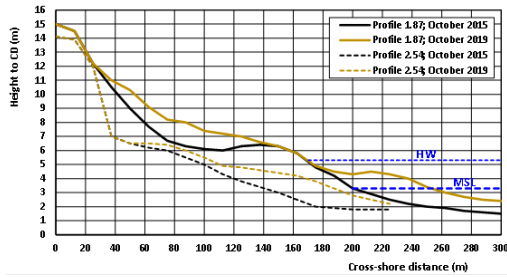


Figure 7. Beach profiles at PK 1.87 and 2.54; 2015 and 2019.

4.4. Longshore Sand Transport Computations and Coastline Changes

Two methods have been used to compute the LST at various locations along the coast between Négade and Barriquand: 1) LONGMOR-model and 2) detailed CROSMOR-model.

4.4.1. LONGMOR-Model Results

Figure 8 shows the computed LST values by van Rijn as function of the shore normal angle to north (defined as the angle of vector from sea to land)^[17]. The LST values are based on the offshore (at 20 m) wave climate with 59 conditions. The sand diameter is $d_{50} = 0.35$ mm. The beach slope is set to 1 to 100. The net LST (NALT) is maximum about 1.5 million m^3 /year to north for an angle of 125° (close to Barriquand). Including the tidal current (0.3 m/s in the surf zone), the NALT to north is much smaller as the LST to south is much higher due the tidal current to south. The results clearly indicate that the north-going LST is dominant for angles $> 90^\circ$ (north of Point Négade). The south-going LST values are only substantial for angles $< 90^\circ$ (south of Point Négade). It should be realised that the LST-values represent sand transport capacity values. The actual LST values are smaller due to the presence of structures and limited availability of sand.

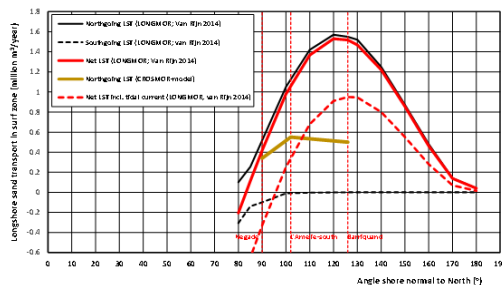


Figure 8. Longshore sand transport at locations north of Point Négade, LONGMOR; $d_{50} = 0.35$ mm.

4.4.2. CROSMOR-Model Results

The CROSMOR-model has been applied for seven wave cases and four locations (beach profiles of Barriquand-northwest, L'Amélie-north, L'Amélie-south and Négade). The sand diameter is $d_{50} = 0.35$ mm. The bed roughness is 0.03 m. Model runs with and without tidal currents have been made (flood of +0.3 m/s to north and ebb of -0.3 m/s to south) both for HW (+1.7 m above MSL) and LW (-1.7 m). The effect of the tide level on LST is small. The model results with tidal currents have been used to derive the total sand transport on the shoreface (between -20 m and -5 m) and in the surf zone. Figure 9 shows the cross-shore distribution of wave height, longshore current velocity and sand transport along the Barriquand-profile during HW and LW for waves with an offshore height of $H_{s,0} = 2$ m.

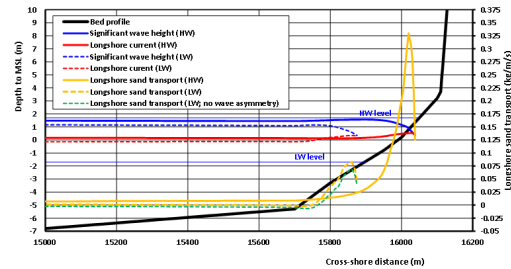


Figure 9. Computed wave height, longshore current velocity and longshore sand transport along cross-shore profile Barriquand-northwest; $d_{50} = 0.35$ mm; $H_{s,0} \approx 2$ m; CROSMOR-model.

Typical results observed in Figure 9 are:

- longshore current during LW is to south on the shoreface (< -5 m) and gradually decreases in landward direction due to bed friction; maximum longshore current in the surf zone during LW is 0.35 m/s to north (change from south to north near the shore); and 0.55 m/s to the north during HW;
- LST on the shoreface is to the north during HW;
- LST on the shoreface is also to the north during LW when the longshore current is to the south; wave asymmetry generates a relatively strong north-going bed load transport; longshore transport on the shoreface is to south when wave asymmetry effects are neglected;
- LST in the surf zone is relatively high and to the north (waves from south-west).

The computed LST values in the surf zone (landward of -5 m; width ≈ 250 m) are:

Barriquand: LST is 0.5 million m^3 /year to north in-

creasing to 1.2 million m^3/year incl. tidal current;

L'Amelie-north: LST is 0.55 million m^3/year to north increasing to 0.92 million m^3/year incl. tidal current;

L'Amelie-south: LST is 0.55 million m^3/year to north increasing to 0.7 million m^3/year incl. tidal current;

Négade: LST is 0.35 million m^3/year to north increasing to 0.4 million m^3/year incl. tidal current.

4.4.3. Best Estimate of Longshore Sand Transport

The results of the LONGMOR and CROSMOR models indicate values in the range of 0.3 to 0.7 Mm^3/year in the surf and shoreface zone between Négade and Barriquand. The LST values of the CROSMOR-model are more realistic than the values of the LONGMOR-model, as the actual cross-shore bottom profile is taken into account. The CROSMOR-model also produces LST-values in the shoreface zone. Based on this, the best estimate of the LST is shown in **Figure 10**. The north-going LST in the surf zone increases from south to north due to an increasing wave incidence angle with respect to the coastline angle. South of Négade is a point of zero LST (divergence point or null point). It should be realised that the values given in **Figure 10** for the surf zone are sand transport capacity values in conditions with unlimited supply of sand (long and straight beaches; wide and high beaches; multiple breaker bars). Most of the sand supply comes from dune erosion in two regions: Négade-L'Amelie (1.5 km) and L'Amelie-Camping LS (1.5 km). The actual NALT in the surf zone at Soulac beach is unknown, but it is less than the LST capacity and is estimated to be about $300,000 \pm 150,000 \text{ m}^3/\text{year}$.



Figure 10. Net annual longshore sand transport values in shoreface zone (seaward of -5 m depth) and in surf zone (landward of -5 m depth line).

4.5. Coastline Hindcast 2014–2021

The LONGMOR-model with the LST-equation of van Rijn has been used to hindcast the coastline changes between 2014 and 2021 after extension (with 80 m) of the Barriquand groyne^[17]. The model domain extends over about 6 km south of the Barriquand groyne. The tip of the Barriquand groyne is landward of LAT-line (about 2.5 m below MSL). The sand diameter is $d_{50} = 0.35 \text{ mm}$. The angle between the main wave direction and the shore normal varies between 15° (L'Amelie at $x = 0 \text{ m}$) and 30° (Barriquand $x = 4500 \text{ m}$).

The two most important parameters are the net annual LST (NALT) and the percentage of bypassing sand transport (BPP) over and along the tip of the groyne. Based on Section 4.4.3, the NALT is in the range of $150,000 \text{ m}^3/\text{year}$ landward of LAT-line (active layer = 5 m) to $450,000 \text{ m}^3/\text{year}$ landward of -5 m depth line below MSL (active layer of 10 m). The BPP is estimated to be in the range of 40% to 75%, as the existing groyne is situated landward of the LAT depth contour, whereas the surf zone extends to the -5 m depth contour. Furthermore, sand will be carried over the groyne during storm conditions.

The detailed coastlines (MSL, HAT, LAT, 5 m depth) of 2014, 2017 and 2020 are shown in **Figure 11**. The origin ($x = 0$) is the groyne north of L'Amelie. The model was calibrated by varying the K-coefficient of the LST in the active layer of 5 m (between LAT and HAT)^[17]. Detailed model runs have been made with and without local sand replacements (excavation near Barriquand and dumping of beach sand near Camping LS; about $200,000 \text{ m}^3$ of sand between 2018 and 2021).

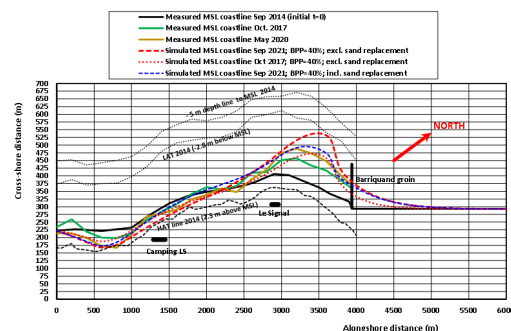


Figure 11. Computed coastline changes in region Soulac, 2014–2021; detailed calibration LONGMOR.

Figure 11 also shows hindcasted MSL-coastlines between 2014 and 2021 excluding and including local sand

replacements. The best results are obtained for NALT = 180,000 m³/year to north at x = 0. The computed results of **Figure 11** are:

- between L'Amélie (x = 0 m) and Camping LS: major erosion of about 300,000 m³ over 7 years including sand replacements;
- between Le Signal and Barriquand-groyne (x = 2200 to x = 3700 m): deposition of sand (about 600,000 m³ over seven years excluding sand replacements;
- north of the Barriquand-groyne: deposition of about 125,000 m³ over seven years due to bypassing.

Figure 12 shows the NALT landward of the LAT-line and averaged over the period September 2014 to September 2021. The NALT at the origin is about 180,000 m³/year which increases to 250,000 m³/year around Le Signal and decreases to 110,000 m³/year between Le Signal and Barriquand groyne (x = 2500 to 4000 m). The bypassing longshore transport is about 110,000 m³/year, which is about 45% of the updrift value of 250,000 m³/year. The increase of NALT between x = 0 and x = 2200 m is caused by the change of the coastline north of L'Amélie with respect to the coastline south of L'Amélie. The overall NALT-value over the length of the domain decreases by about 70,000 m³/year or a total net deposition volume about 490,000 m³ over seven years.

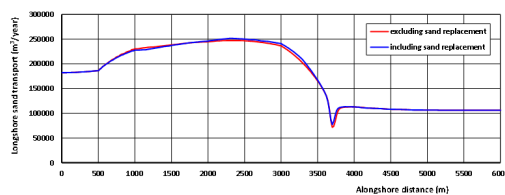


Figure 12. Computed longshore sand transport landward of the LAT-line; LONGMOR-model.

Overall, there is net deposition volume between x = 0 and x = 6000 m of about 600,000 + 125,000 – 300,000 = 425,000 m³ over 7 years or about 60,000 m³/year which is about equal to the difference (180,000–110,000 m³/year) in LST between x = 0 and x = 6000 m (**Figure 12**).

The maximum predicted accretion including sand replacement is about 100 m at x = 3500 m over 7 years. The MSL line is far seaward of the tip of the groyne at that location (x = 3500 m). The replacement of sand from the section 3300–3800 m to the section 1150–2300 m in the period 2018 to 2021 mitigates the erosion around Camping LS. Based on these results, the NALT at Soulac is estimated to be of the

order of 200,000 50,000 m³/year landward of the LAT-line.

4.6. Proposed Solutions for Region of Soulac Sur Mer

The coastal section near Soulac is characterised by: a) north-going sand transport capacity in the surf zone; b) severe erosion of beaches and dunes; c) limited availability of sand (null point about 1 to 2 km south of Négade); and d) HW line is situated almost up to dune foot (small dry beach). The most sustainable solution is the design and construction of a new groyne updrift of the Barriquand groyne. The most realistic location for the construction of a new groyne is the urbanised coastal section (Boulevard des Dunes) between Camping LS and Le Signal. The detailed coastlines (MSL, HAT, LAT, 5 m depth) of 2014, 2017 and 2020 are shown in **Figure 13**. The predicted coastlines are shown for three cases with different values of BPP. The origin (x = 0) is the groyne north of L'Amélie. The model was calibrated by varying the K-coefficient of the LST in the active layer of 5 m (between LAT and HAT)^[17]. Beach nourishments or sand replacements are excluded. The NALT at x = 0 m is 180,000 m³/year (d₅₀ = 0.35 mm). The input data and settings are similar to those of the calibration runs.

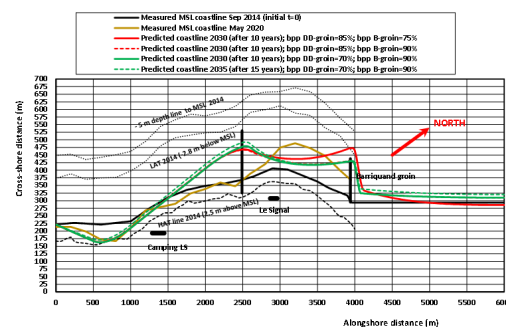


Figure 13. Predicted coastline development in the period 2020–2035; LONGMOR-model.

Figure 14 shows the NALT. The total volume of sand deposited in the total domain of 6 km is 180,000–145,000 = 35,000 m³ per year, or about 350,000 m³ over 10 years. This low trapping value is caused by the relatively high bypassing percentages. The most important results are (**Figure 14**):

- coastal accretion of about 300,000 m³ over ten years southward of the new groyne;
- erosion of sand of about 150,000 m³ over ten years in the middle part between the new groyne and the Barriquand groyne; accretion of about 150,000 m³

over ten years at both ends of the compartment between the two groynes; sand volume between groynes is redistributed;

- coastal accretion of about 75,000 m³ over ten years northward of the Barriquand groyne.

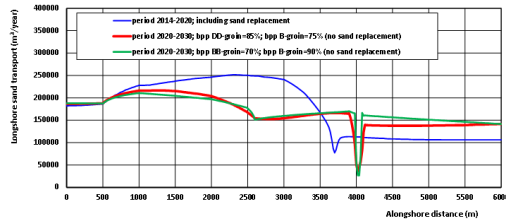


Figure 14. Computed annual-averaged longshore sand transport (NALT) landward of the LAT-line.

Another solution may be a large-scale beach nourishment north of Camping LS and South of Le Signal (2.3 million m³; 150 m into sea; alongshore = 1500 m; layer thickness = 10 m). **Figure 15** shows the predicted coastline after 10 years for 2 cases with NALT = 200,000 m³/year (active layer = 5 m) and 450,000 m³/year (active layer = 10 m) to north, sand $d_{50} = 0.35$ mm and BPP = 80%. The sand trapping updrift of Camping LS is about 500,000 m³ after ten years. The total erosion of the nourishment area is 1.2 million m³ after 10 years. The total deposition between the nourishment area and the Barriquand groyne is about 0.3 million m³ after 10 years. The total bypassing around the tip of the Barriquand groyne is about 0.9 million m³ after 10 years (supply for beaches north of Soulac). NALT values in the range of 200,000 to 450,000 m³/year have a minor effect on the erosion of the beach nourishment. The reason for this is that the LST reduces to almost zero if the coastline orientation is normal to the incoming waves (angle of 15° to 20° with coast normal). In reality, the lifetime of the beach nourishment may be much shorter (three to five years) due to cross-shore transport processes. The toe of the nourishment profile will be relatively steep (1 to 10) resulting in higher beach erosion rates, which is not included in the LONGMOR-1D model. Beach nourishments are easy if sand is abundantly available and are always successful in the short term, but repeated nourishments are often required to satisfy long-term objectives.

Overall, it is concluded that the construction of a new beach groyne at Soulac beach is effective for the accumulation (accretion) of beach sand on the updrift side of the groyne, but the groyne should not be too long to allow suf-

ficient bypassing of sand by longshore transport processes. Another solution may be the placement of a large-scale beach nourishment, but this has to be repeated regularly (every five to ten years). An economic evaluation should be made to find the most economic long-term solution.

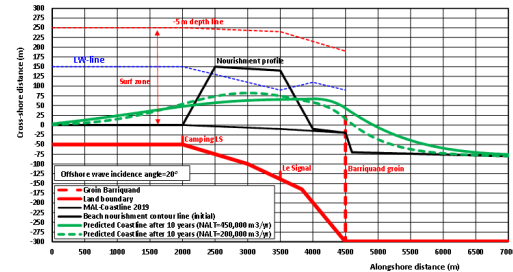


Figure 15. Predicted coastline development in period 2019–2029; $d_{50} = 0.35$ mm.

Basic guidelines are: 1) determine representative annual wave climate; 2) determine nearshore tidal current velocities; 3) determine NALT due to waves and currents from empirical LST-equation; 4) use cross-shore sand transport model (CROSMOR) to include the effect off the cross-shore bed profile on LST; 5) calibrate 1D coastline model (LONGMOR) using observed coastline changes (hindcast); 6) apply calibrated coastline model for computation of future coastline changes; 7) take measures to mitigate downdrift erosion.

5. Example Case: Modelling of Coastline Changes around Long Harbour Breakwater; Lagos, Nigeria

5.1. General

This example case refers to the modelling of the accretion updrift of long harbour groynes and the downdrift erosion due to blocking of the LST. Various structures have been designed and built to defend the downdrift coast.

5.2. Site Description

The coastlines on both sides of the Lagos harbour entrance are fairly straight (**Figure 16**). The harbour breakwaters were built between 1908 and 1912. The east coast in 2000 lies about 3 km inland from the tip of the eastern harbour breakwater. The beach of the east coast is a low-lying sandy beach with a maximum crest elevation of 2.5 to 3 m above MSL and a beach width of 50 to 100 m. Lagoons

are present behind the barrier complexes, separated from the ocean by a narrow strip of land. The navigation channel has depths of 15 to 25 m between the breakwater tips; the water depth is about 15 m outside the breakwater tips. Since 2010, the area east of the breakwater has been reclaimed land over 6 km^[37].

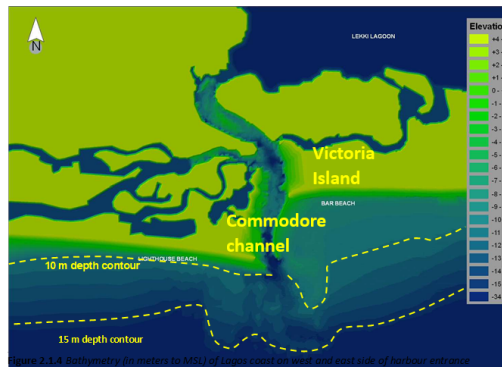


Figure 16. Bathymetry (in m MSL) on west and east sides of harbour entrance (before land reclamation).

5.3. Environmental Conditions

Semi-diurnal tides are present along the Lagos coast. The mean spring tidal range is about 1 m, while the neap tidal range is 0.5 m. Extreme spring tidal range is 1.3 m (1.8 above CD). MSL is 0.46 m above CD.

Storm surge levels due to extreme onshore wind conditions can be 1 to 2 m above the normal level, depending on meteorological conditions in August. The maximum stormwater level above CD is approximately 3 to 4 m above CD^[38–41]. Flooding of the Victoria Island by storm surges is observed every year. Beach ridge erosion is large during these conditions. The ocean current in front of the West African coast is the Guinea Current, flowing eastward in front of the West African coast. In summer (May–September), the Guinea Current is strongest with velocities of about 1 m/s and up to 0.5 m/s in other periods. Peak tidal currents are about 1 m/s in the mouth of the main inlet.

The general wind pattern is from southwesterly directions during the rainy season and from the northwesterly directions during the dry season (late October to early March).

The beaches are exposed to high-energy waves. Swell waves with periods up to 20 s are dominant, superimposed by wind waves with periods between 3 and 8 s. Observations show that the waves break (plunging breaking waves) at oblique angles of 3 to 13 degrees at depths of 2 to 3 m

at about 50 to 100 m from the shoreline. These breaking waves with heights between 0.5 and 2 m generate alongshore currents of about 0.5 to 1.3 m/s in an eastern direction (from West to East). The two dominant wave directions are 180° and 210°. Significant wave heights during fair weather conditions are typically between 1 and 2 m (periods 10 to 12 s). The number of storms per year varies from 1 to 5. Generally, the largest waves do occur in August (2.2 m in 1997 to 3 m in 2014).

The morphological system of the Lagos coast is dominated by straight barriers/ridges and lagoons^[42, 43]. The coast on the west side of the harbour entrance shows massive accretion over time as the net annual longshore transport (NALT) is blocked by the harbour breakwater. The difference in coastline position on both sides of the breakwater was about 500 m in 1910 and about 1000 m in 2010^[43]. The accretion on the west side of the breakwater was of the order of 500 m over 100 years (1910 to 2010). The erosion on the east side of the harbour breakwater was also of the order of 500 m in the same period or about 5 m/year^[43]. The coastal recession on the east side extends over a distance of 10 to 15 km. Substantial beach nourishments up to 28 million m³ were executed to mitigate erosion on the east side^[41, 43]. No hard structures were used before 2015 to reduce the coastal recession. Recently (around 2015), several groynes were constructed east of the EKO Atlantic City project (7 km east of breakwater); see **Figure 17**. Some groyne compartments have submerged breakwaters (parallel to the beach) between the tip of the groynes, see lower panel of **Figure 17**. Information on the sediment composition shows values of d_{50} between 0.4 and 1.5 mm^[43]. The sand diameter (d_{50}) is between 0.2 and 0.6 mm; d_{90} is between 0.6 and 1.5 mm. The presence of relatively steep beach slopes is also an indication that the beaches along the east coast consist of coarse sands.

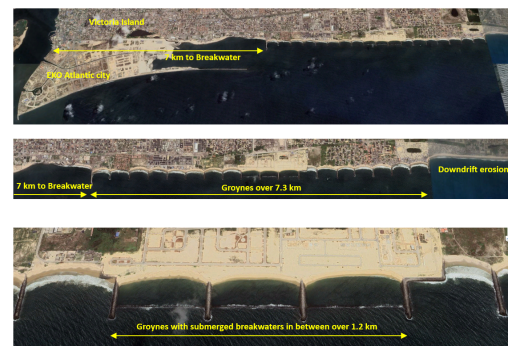


Figure 17. Groyne field on east side of breakwater, Lagos Nigeria.

The net annual longshore transport is of the order of 0.5 million m^3 per year from west to east. The accretion and erosion volumes on both sides of the harbour breakwaters are approximately equal (20 to 24 million m^3). During the period 1960–2010, the total erosion based on coastline recession on the east side is estimated to be about 20 million m^3 , despite a total nourishment volume of about 28 million m^3 with sand from offshore borrow pits. Hence, the total erosion is $20 + 28 = 48$ millions m^3 over the period of 50 years resulting in a longshore transport rate of 1 million m^3 per year. The analysis results for both periods indicate that the bypassing of sand around the harbour entrance is almost zero. Sand trapped in the deep navigation channel is removed by tidal currents (of about 1 m/s) and by dredging activities to maintain the depth of the channel.

Recently (2008) the western breakwater has been extended. In the period 2010–2015, the land reclamation EKO Atlantic City has been built on the east side of the breakwater (Figure 17)^[37]. The coastal recession in the section between 7 and 14 km from the breakwater was about 40 to 50 m in the period 2000 to 2015 or about 3 m per year. To reduce the erosion in this coastal section, a groyne field was built over a distance of 7.3 km in 2015 and 2016. However, the coastal recession in the groyne compartments continued with about 30 m in the period 2015–2024 or about 3 m per year. Hence, open groyne compartments are not very effective along this coast. Submerged breakwaters (crest at 0.5 m below MSL) parallel to the coast were built in three groyne compartments in 2021 and 2022 to further reduce the beach erosion (Figure 17)^[44]. A major problem is the severe downdrift erosion east of the terminal groyne, which is about 200 m between 2015 and 2024 or about 20 m per year.

5.4. Modelling of Longshore Sand Transport

The net annual longshore transport (NALT) along the coast (without any structures) has been computed by the LST-equation proposed by van Rijn using the local wave climate at deep water (30 m)^[17]. The sand diameter is varied in the range of 0.25 and 0.55 mm. The beach slope (β = slope angle) in the surf zone varies between $\tan \beta = 0.015$ and 0.03. The breaker coefficient is set to 0.8 for swswell-type waves.

Figure 18 shows the net annual longshore transport as function of the angle of the coast normal line and the sand

size (d_{50}) and the beach slope. The wave breaking coefficient is $\gamma_{br} = 0.8$. The angle of the coast normal (from sea to land) on the far west and east of the harbour breakwater is about 0° which gives a NALT rate of about 0.75 ± 0.2 million m^3 per year to the east for sand of 0.25–0.55 mm and beach slope of about 0.015. The net longshore transport is about 1 ± 0.2 million m^3 per year to the east for sand of 0.25–0.55 mm and a steeper beach slope of about 0.03. A coastline shift of 1° yields a change of the NALT of about 50,000 m^3 /year. The NALT-values are 5% to 10% smaller for a wave breaking coefficient to $\gamma_{br} = 0.6$.

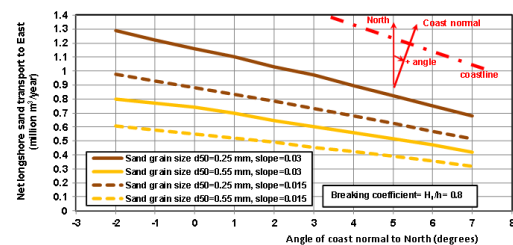


Figure 18. Net annual longshore sand transport as function of coast normal angle and sand grain size; $\gamma_{br} = 0.8$.

The net annual longshore transport consists of two contributions: to east and to west. The component to west due to waves from the south-east is of the order of 10,000 m^3 /year, which is negligibly small.

The computed net longshore transport of 0.75 million m^3 /year to the east is in good agreement with the observed values of 0.75 ± 0.25 million m^3 /year based on the measured coastline accretion on the west side. It is noted that the results of Figure 18 are only valid for annual wave conditions along a straight and open sandy coast without any structures. The actual net longshore transport is smaller due to the presence of hard structures (seawalls, revetments, groynes, etc.), which generally are constructed to reduce the net longshore transport.

5.5. Modelling of Coastline Accretion on West of Harbour Breakwater

The LONGMOR-model has been used to compute the coastline changes over a period of 50 years (1960 to 2010). A simplified wave climate has been used with $H_{s,0} = 3$ m and duration of 25 days per year resulting in a net annual longshore transport of about 500,000 m^3 /year. Figure 19 illustrates the computed coastline changes along the west coast over a 50-year period (1960–2010). The net updrift

longshore transport has been varied in the range of 400,000 to 600,000 m³/year. The active layer thickness has been varied in the range of 10 to 12 m. The bypassing rate at the tip of the breakwater is set to 20% of the updrift value. Measured values of the coastline in 2010 are also shown [43]. The LONGMOR-model produces very reasonable results for a net annual longshore transport of 400,000 m³/year and layer thickness values of 10 to 12 m. The bypassing of sand leads to deposition in the deeper entrance channel, which has to be removed by maintenance dredging. Around 2010, the west breakwater was extended over about 150 to 200 m to reduce the bypassing rate. Based on this, it is most realistic to assume that the supply of sand across the entrance channel to the east coast is almost zero.

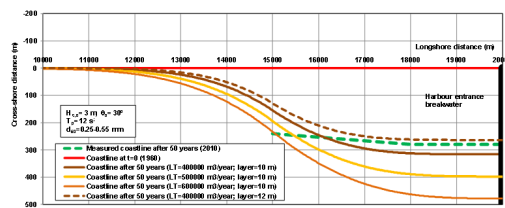


Figure 19. Computed and measured coastline changes on west side during the period 1960 to 2010.

5.6. Modelling of Coastline Erosion on East of Harbour Breakwater (without Land Reclamation)

The coast situated east of the long harbour breakwaters is eroding as a result of the blocking of the LST. The LONGMOR-model has been used to compute the coastline changes at Kuramo beach (at about 3 km from the harbour breakwater) over the period 2005–2010. The effect of the harbour breakwater has been taken into account. The input data are: $d_{50} = 0.55$ mm, beach slope $\tan = 0.015$, breaker coefficient = 0.8, active layer = 10 m. The wave climate in the model was schematized to give a NALT at downdrift end of 650,000 m³/year to east. The DIFSAND-model including diffracted waves in the lee of the breakwater (based on the method conducted by Kamphuis) was used to determine the NALT in the lee zone [32]. An example of the DIFSAND-model is given in **Figure 20** showing the wave and current parameters at the beach of Kuramo Waters for a storm event with $H_{s,0} = 4$ m. The wave height at the breaker line varies from $H_{s,br} = 2.2$ m at $x = 0$ m to $H_{s,br} = 3.4$ m outside the diffraction zone ($x > 3$ km). Near the breakwater, the long-

shore current is towards the structure. At Kuramo beach, the longshore current velocity increases from 0.55 m/s to 0.7 m/s in an eastward direction.

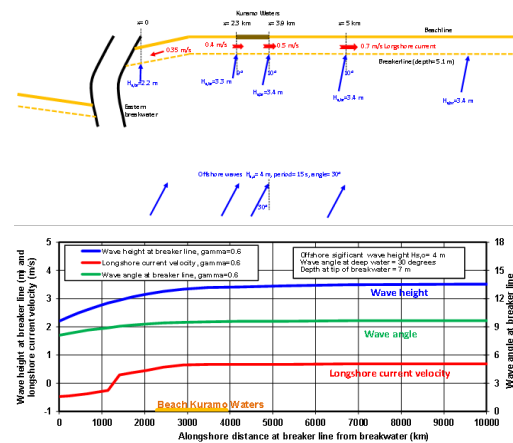


Figure 20. Hydrodynamic parameters for $H_{s,0} = 4$ m from South-West ($\gamma_{br} = 0.6$); DIFSAND-model; no land reclamation.

Figure 21 shows the computed longshore transport of the DIFSAND-model for $H_{s,0} = 3$ and 4 m, offshore angle = 30° (waves from south-west), $d_{50} = 0.55$ mm and slope = 0.015. Far away (east) from the harbour entrance channel, the longshore transport is about 6100 m³/day for offshore waves of 3 m.

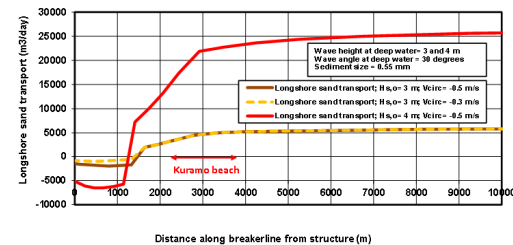


Figure 21. Longshore transport in m³/day along Kuramo beach and surrounding coastlines based on DIFSAND-model; no land reclamation; $d_{50} = 0.55$ mm, $H_{s,0} = 3$ and 4 m from south-west.

Figure 22 shows the computed coastline of the LONGMOR-model after five years (2005 to 2010 before the construction of the land reclamation). The measured beach recession at Kuramo (small beach ridge-lagoon system) is about 25 m over 5 years (2005–2010). Two values of the NALT have been used: 1) high estimate of the net annual longshore transport LST = 650,000 m³/year (at the far end $x = 15$ km east of the harbour breakwater) and 2) low estimate of the net annual longshore transport LST = 300,000 m³/year.

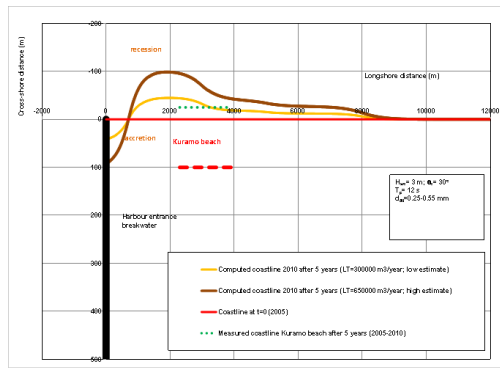


Figure 22. Coastline along Kuramo beach and surrounding coastlines (LONGMOR-model); no land reclamation; $d_{50} = 0.25\text{--}0.55$ mm, $H_{s,0} = 3$ m from South-West.

The best agreement with measured coastal recession at Kuramo beach (about 25 m over 5 years or 5 m/year) is obtained for a value of $300,000\text{ m}^3/\text{year}$. The alongshore scale of the coastal erosion on the east coast is of the order of 10 km. The net annual longshore transport rate to simulate the coastal recession rates at Kuramo beach before the construction of the land reclamation correctly is of the order of $300,000\text{ m}^3/\text{year}$, which is considerably less than the value of about $500,000$ to $900,000\text{ m}^3/\text{year}$ derived from the long-term historical coastline recession rates of the east coast. Most likely, the present recession rates are smaller than the older recession rates due to the presence of local coastal defence structures (revetments and short groynes) and local beach nourishment schemes.

Overall, it is concluded that the blocking of longshore transport by the harbour breakwaters leads to large-scale coastal accretion on the updrift (west) side of the breakwaters, which can be rather well represented by 1D numerical coastline modelling. Substantial beach erosion has occurred on the downdrift (east) side in the lee area of the breakwaters. A large-scale land reclamation project (EKO Atlantic City project) has been executed in the lee zone area resulting in an eastward shift of the downdrift erosion zone. To mitigate the ongoing beach erosion on the east side, a series of beach groynes has been built along the most populated coastal region. At some sites, submerged breakwaters have been built between the tips of the groynes to completely stop the beach erosion. However, beach erosion due to longshore transport processes continues east of the last groyne, which can only be mitigated by regular beach nourishment.

Basic guidelines are: 1) determine representative annual wave climate; 2) determine nearshore tidal current ve-

locities; 3) apply detailed wave model to compute the wave height and wave direction in the diffraction zone in the lee of the structure (breakwater); 4) determine NALT due to waves and currents along the coast from empirical LST-equation; 4) use cross-shore sand transport model (CROSMOR) to include the effect off the cross-shore bed profile on LST; 5) calibrate 1D coastline model (LONGMOR) using observed coastline changes (hindcast data); 6) apply calibrated coastline model for computation of future coastline changes; 7) takes measures to mitigate downdrift erosion.

6. Example Case: Modelling of Erosion in Groyne Compartments, Black Sea Coast, Romania

6.1. General

This example case refers to the construction of artificial beaches (beach fills) between coastal groynes and the modelling of the erosion of the beach fills inside the groyne compartments. The cross-shore bed profile of a beach fill is mostly much steeper than the natural bed profile resulting in increased wave attack and associated erosion of sand. Cross-shore modelling of the beach erosion is applied and the model results are used to estimate the lifetime of the beach fills and the required beach maintenance volumes involved. It may be attractive to build a submerged (detached) breakwater between the groynes to reduce the loss of sand from the beach zone to deeper water, which is also studied herein.

6.2. Site Description

Coastal works along the Romanian Black Sea coast involve: 1) the construction of several straight and T-head groynes with lengths between 400 and 700 m and spacings of 500 to 1000 m and 2) the placement of beach sand (nourishment volume of 500 to $1000\text{ m}^3/\text{m}$) in the compartments between the groynes.

6.3. Environmental Conditions

The tidal range is 0.1 m. The annual wave climate at -10 m depth is schematised into ten wave conditions with waves of 0.6 to 2 m and wave angles between 20° and 30°

to the shore normal.

The beach slope is assumed to be 1 to 20. The wave runup level including tide and surge is about 1.7 m above SWL (still water level) during annual wave conditions^[45]. The wave runup is about 3.5 for extreme conditions ($H_{s,0} = 8$ m, $T_p = 15$ s, once per 100 years).

The nourished beach profile (sand with $d_{50} = 0.2$ mm) between the straight groynes consists of: a) flat upper beach crest at about 3 to 3.5 m; b) beach slope of 1 to 20 above SWL (beach length of 60 to 70 m); c) seabed slope of 1 to 60 between SWL and -4 m depth; d) transition slope of 1 to 15 between -4 m and -6.75 m depth at seaward end of nourishment zone; and e) seabed slope of 1 to 125 between -6.75 m and -30 m. It is noted that this nourishment profile is an artificial profile consisting of a combination of straight profiles and is not an **equilibrium** beach profile and will, therefore, be modified over time by cross-shore sand transport processes into a more natural profile in dynamic equilibrium with the local wave climate.

6.4. Cross-Shore Modelling Results

The following CROSMOR-runs have been made to estimate the loss of sand from the groyne cells: i) annual runs over 1 year; ii) short-term runs over 1 day for storms with return period of 1 to 100 years; and iii) long-term runs with a series of 60 storm events with return periods between 1 and 100 years, representative for a period of 50 years. The basic input data of the CROSMOR-model are: $d_{50} = 0.2$ mm, water temperature = 20° , wave asymmetry based on Isobe-Horikawa 1982^[22].

6.4.1. Beach Erosion Due to Annual Waves

Figure 23 shows the computed beach profiles after one, three and five years for an annual wave climate plus a storm with a return period of 1 year. The beach erosion volumes are given in Table 2. The erosion volumes and beach recession values are largest during the first year when the breaker bar is formed. The breaker bar generated at the toe of the nourishment zone (around $x = 3200$ m) becomes a focus point for wave breaking and thus protects the beach against extreme erosion. The breaker bar grows by onshore-directed transport and erosion at the seaward flank due to shoaling waves and offshore-directed transport and erosion on the landward flank of the bar due to breaking waves plus return

currents (see yellow arrows in Figure 23).

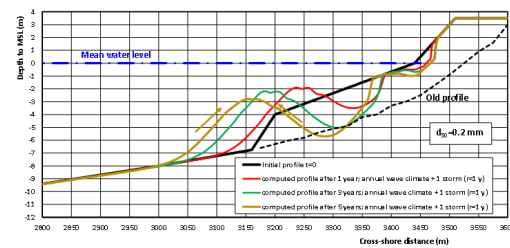


Figure 23. Computed beach profiles for one to five years for annual wave climate.

Onshore transport in the zone between -1 and -3 m may also occur during conditions with low waves, but this effect is overruled by seaward transport due to higher waves resulting in net erosion in this zone. The time scale of bar generation is of the order of 0.5 to 1 year based on the CROSMOR-results. The bar migrates slowly in a seaward direction. The height of the offshore breaker bar is overestimated (by about 30%) by the CROSMOR-model as various smoothing effects are not taken into account (alongshore transport gradients and redistribution of sand within the compartment between the groynes). A fairly stable terrace with a length of about 50 m is formed in the nearshore zone (at depth of about -0.5 m). The beach face is steepening in the zone above -1 m SWL (Still Water Level) due to erosion processes. Terrace formation and beach face steepening (even beach scarping) are typical features after nourishment at sites with a constant water level (lakes, non-tidal seas). The nearshore terrace may also move onshore during a long period with very low waves < 0.6 m (neglected in these simulations). The seabed below -8 m is stable (no movement). The predicted beach erosion above -1 m SWL after five years is about $100 \text{ m}^3/\text{m}$ or $20 \text{ m}^3/\text{m}/\text{year}$ (Table 2).

6.4.2. Short-Term Beach Erosion Due to Storms

To quantify the beach erosion due to extreme storms with a duration of 1 day (24 hours), the following CROSMOR runs have been done using the initial beach profile of Figure 24:

- A1; storm with return period of 1 year: $H_{s,0} = 3.5$ m at -30 m, $T_p = 9$ s, $\theta_0 = 20^\circ$, storm setup = 0.6 m;
- A2; storm with return period of 10 years: $H_{s,0} = 5.8$ m at -30 m, $T_p = 10$ s, $\theta_0 = 20^\circ$, storm setup = 0.7 m;
- A3; storm with return period of 25 years: $H_{s,0} = 6.6$ m at -30 m, $T_p = 11$ s, $\theta_0 = 20^\circ$, storm setup = 0.8 m;

Table 2. Predicted erosion and recession values (R.P. = Return Period; SWL=Still Water Level).

Case	Wave Climate	Nearshore Erosion between -4 m and -1 m SWL	Nearshore Erosion above -1 m SWL	Beach Recession	Beach Recession at SWL+2
Annual	Annual waves+1 storm	130 m ³ /m after 1 year	40 m ³ /m after 1 year	25 m after 1 year	0
Short-term storms	A1; R.P. = 1 year	70 m ³ /m after 1 day	2 m ³ /m after 1 day	1 m after 1 day	0
	A2; R.P. = 10 years	100 m ³ /m after 1 day	5 m ³ /m after 1 day	2 m after 1 day	0
	A3; R.P. = 25 years	130 m ³ /m after 1 day	15 m ³ /m after 1 day	10 m after 1 day	0
	A4; R.P. = 50 years	140 m ³ /m after 1 day	20 m ³ /m after 1 day	15 m after 1 day	0
	A5; R.P. = 100 years	150 m ³ /m after 1 day	45 m ³ /m after 1 day	25 m after 1 day	25 m after 1 day
Long-term	Series of 60 storms (30 days) representative for 50 years; duration of storm = 12 hrs	250 m ³ /m after 50 years	220 m ³ /m after 50 years	60 m after 50 years	30 m after 50 years

- A4; storm with return period of 50 years: $H_{s,0} = 7.4$ m at -30 m, $T_p = 13$ s, $\theta_0 = 20^\circ$, storm setup = 0.9 m;
- A5; storm with return period of 100 years: $H_{s,0} = 8.0$ m at -30 m, $T_p = 15$ s, $\theta_0 = 20^\circ$, storm setup = 1.05 m.

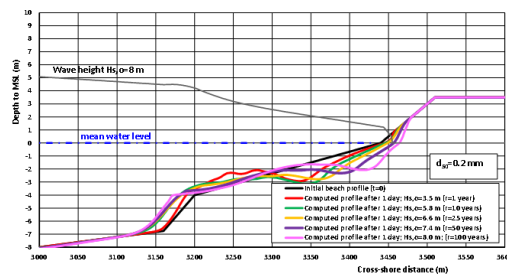


Figure 24. Computed beach profiles for extreme storms with duration of 1 day.

Figure 24 shows the computed profiles after 1 day. Most changes occur in the nearshore nourishment zone (landward of $x = 3100$ m). Minor changes occur at the seabed seaward of $x = 3100$ m. The onset of breaker bar formation occurs between $x = 3150$ and 3300 m. Minor storms create a breaker bar in the nourishment zone, whereas major storms carry most of the sand to the toe of the nourishment zone. The beach erosion above -1 m SWL is in the range of 2 to 45 m³/m after 1 day. The maximum beach recession at the still-water line is approximately 25 m after 1 day. The beach erosion is rather high (20 to 45 m³/m after 1 day) for the highest storm with return periods of 50 to 100 years and a setup of the order of 1 m. The total erosion is much higher (about 150 m³/m after 1 day). It is noted that the modelled storm waves are assumed to have an offshore incident wave angle of 20° to the coast resulting in relatively strong wave-driven longshore currents in the nearshore zone. These wave-driven

currents cannot fully develop inside the groyne cells resulting in lower sand concentrations and transport and thus in lower beach erosion rates.

6.4.3. Long-Term Erosion Due to Annual Waves and Storms

Long-term runs over a time scale of 50 years cannot yet be made by using the CROSMOR-model, because this leads to unrealistic results as the (smoothing) effects of alongshore transport processes are not included. Therefore, a schematised approach has been used, as follows: model runs with 50 minor storms and 10 major storms. The storm details are: 50 storms with return period = 1 year; 6 storms with return period = 10 years, two storms with return period = 25 years, one storm with return period = 50 years and one storm with return period = 100 years. Each storm has a duration of 12 hours. The storm surge level above MSL varies between 0.6 m and about 1 m. **Figure 25** shows the computed beach profiles for these 60 storm events, which are representative for a period of 50 years. Beach erosion and beach recession are given in **Table 2**. The total beach erosion is about 500 m³/m after 50 years. The beach recession is a maximum of 60 m at SWL and 30 m at +2 m SWL. The beach profile above -2 m SWL is completely eroded away.

The eroded sand is deposited at offshore breaker bar locations between -8 m and -10 m SWL. The computed bars are somewhat peaked due to the onshore transport at the seaward flank. The predicted beach erosion results are conservative values, as a storm duration of 12 hours is fairly long (mostly six to 12 hours). Furthermore, it is noted that a sequence of 60 successive storms is too conservative because the beach recovery due to daily waves in between the storm

events is not included. In practice, a beach terrace in the zone between -1 and -2 m will be present creating a sand buffer for the stormy seasons.

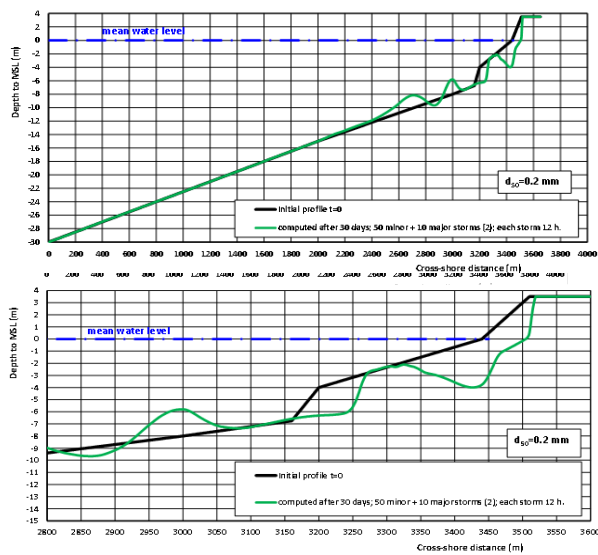


Figure 25. Computed beach profiles for 60 storms representative for a period of 50 years.

The beach erosion can be substantially reduced by placing a submerged breakwater with high crest at -0.5 m below mean water surface level between the groynes, as shown in **Figure 26** (same wave climate)^[46]. Including the storm surge level, the water depth above the crest varies in the range of 1 to 1.5 m which means that waves higher than 1.5 m cannot pass the crest due to wave breaking on the crest. The beach erosion is reduced to about 50 to 100 m^3/m for a period of 50 years. The eroded sand is deposited on the seaward flank of the submerged breakwater, but in reality, it will be spread out over a larger distance by violent wave-breaking processes on the seaward flank (not included in the model).

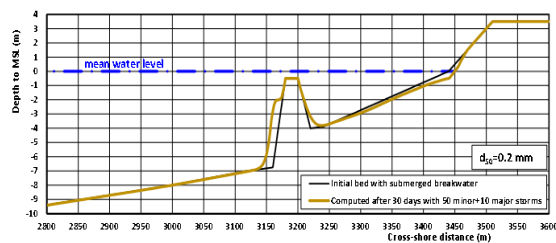


Figure 26. Computed beach profiles for 60 storms representative for a period of 50 years; Effect of submerged breakwater on beach erosion (file: RLOT8SM.inp).

6.5. Long-Term Beach Behaviour and Economic Evaluation

The Black Sea coast near Constanta in Romania is a typical eroding coast with high potential for beach recreation. To mitigate beach erosion, a series of beach groynes has been built recently along the coast. Beach fills are placed inside the compartments (creation of artificial beaches) to increase the beach width for recreational purposes, but the beach fill sand may be gradually eroded from the open groyne compartments by cross-shore transport processes.

To maintain sufficient beach width in the long term, two options are available:

- regular beach nourishment inside each compartment (every 5 to 10 years) to maintain the beach width;
- the construction of submerged breakwaters between the tip of the groynes to prevent erosion of sand from the compartments.

Overall, a beach fill between straight groynes (open cells) along the Black Sea coast has a maximum lifetime of about 25 to 50 years without maintenance activities. In that period of 25 to 50 years, the total computed beach erosion due to cross-shore processes is of the same order (about 500 m^3/m) as the initial beach fill volume (500 to 1000 m^3/m). Beach maintenance of the order of 150 to 300 m^3/m every 5 to 10 years is sufficient to maintain a beach width of 60 m between 0 and +3 m SWL. Given a unit price of \$10 per m^3 for beach fills, the total beach maintenance costs for seven beach fills of 300 m^3/m over 50 years are $7 \times 300 \times 10 = \$21,000$ per meter (alongshore) coastline. The construction of a submerged breakwater between the tip of the groynes reduces both the cross-shore and longshore transport processes, creating a stable beach in the long term. However, the beach stability strongly depends on the crest level of the breakwater between the tips. In the case of oblique waves passing over the breakwater, wave-driven longshore currents will be generated inside the groyne compartments. In addition, updrift/downdrift movement of sand by circulation currents generated by wave diffraction and setup differences may also occur. As a result, the beach inside the groyne compartment will slowly readjust its orientation to arrive at a beach line as much as possible perpendicular to the main wave direction, which is known as equilibrium beach development. Circular or spiral-type beach curves are generally generated in the corner areas of the groynes. The LST is substantially reduced

when a submerged breakwater is present. **Figure 27** shows the effect of a submerged breakwater at depth of 7 m on the annual LST in the case of a severe wave climate (exposed coast). The crest level is varied between -7 m (below the water surface) and $+1$ m (above the surface). The ratio of the LST with and without a submerged breakwater is plotted as function of the ratio of the water depth above the crest of the structure and the water depth without the structure. The LST is reduced to 25% of the original value (without structure) for a submerged crest level at -0.7 m (relative $0.7/7 = 0.1$, on horizontal axis). The LST is minor when the crest of the breakwater is above the water surface (emerged structure). Thus, the crest of the submerged breakwater should be as high as possible to reduce the LST at the beach as much as possible. However, the construction of a submerged breakwater is rather expensive and may not be cost-effective in an economic sense. The construction costs of a submerged breakwater are of the order of \$15 million per kilometer (\$15,000 per meter coastline), which is less than the long-term costs of regular beach maintenance, which are about \$21,000 per meter coastline. Hence, it may be worthwhile to explore the possibility of a permanent submerged breakwater by detailed studies to substantially reduce the beach erosion and thus the maintenance costs^[46].

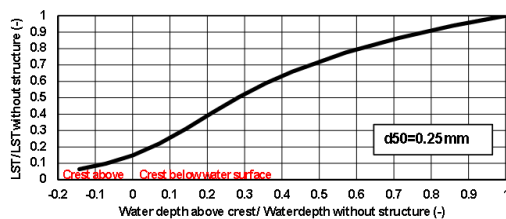


Figure 27. Relative LST as function of relative water depth above crest (depth at structure = 7 m).

Basic guidelines for the design of artificial beaches between groynes are: 1) determine representative annual wave climate; 2) apply cross-shore model (CROSMOR) to determine the transport of sand from the beach zone to deeper water (loss of sand) for the case with and without submerged detached breakwater; 3) estimate the maintenance volume of sand for the case without submerged breakwater; 4) make economic evaluation whether the construction of a detached breakwater is more attractive than regular beach nourishments.

7. Discussion, Conclusions, Guidelines and Recommendations

Many coastal sites suffer from chronic erosion resulting in narrow and steep beaches which are not very suitable for beach recreation. Increased (accelerated) sea level rise due to climate change will enhance coastal erosion demanding global attention and quick responses (intervention schemes and strategies) of coastal engineers and policy makers.

Eroding beaches are generally mitigated by soft beach nourishments (fills) and/or hard structures. Groynes are the most classical structures for coastal protection against erosion. Groynes are relatively simple structures to build. Groynes are mostly built along sandy coasts near inlets with substantial LST and chronic erosion larger than about 2 m/year. Groynes in macro-tidal conditions should be built between the dune foot and the LW-line. The crest level near the dune foot should be around $+3$ m above MSL (Mean Sea Level) and around $+1.5$ m at the seaward end, so that sand can bypass around the tip of the groynes.

Erosion downdrift of the terminal beach groyne is a serious problem due to (partial) blocking of the LST. It is important that beach groynes are designed with sufficient bypassing capacity to reduce the downdrift erosion processes (Soulac example). In mild wave conditions with low LST, the bypassing of longshore transport can also be achieved artificially by a permanent sand transfer plant (South-East Florida coast), but these operations are hardly feasible along a high-energy coast with high LST^[47]. The erosion along these latter types of coasts is mostly mitigated by regular beach nourishments within a framework of intervention schemes (master plans) made by policymakers.

Beach groynes can reduce the chronic erosion along the coast, but open groynes cannot stop the erosion completely because sand can be removed from the groyne compartments by cross-shore processes, particularly in the case of beach fills with relatively steep initial beach profiles (Romania example). Regular beach maintenance (nourishments) in the groyne compartments is required to keep sufficient beach width for recreation. If open groyne compartments do not work well (ongoing erosion), several options are available for improvement (**Figure 28**):

A. regular beach fills in the groyne compartments, which may be problematic if sand is scarce (expensive);

B. construction of T-head or L-head groynes;

C. construction of submerged breakwater between the groynes with crest at -0.5 m below MSL (Lagos coast)^[44, 46], mainly suitable in micro-tidal conditions;

D. construction of revetment at upper beach (slope 1 to 3; crest at $+5$ m) between the groynes.

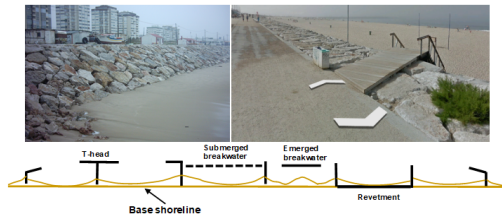


Figure 28. Coastal protection.

Options B and C are good measures to protect the beach inside the compartments by reducing the wave energy penetrating into the compartments, but these options are relatively expensive, particularly when rock material is not locally available.

Option D, which is less expensive, can be used when beach erosion has to be stopped completely (**Figure 28**). Generally, the beach width at the toe of the revetment will be relatively small or absent. A flat area for recreation can be made landward of the revetment crest (top) or regular beach fills protected by short groynes (150 m; spacing 300 m) can be placed at the toe of the revetment. Access to the low-lying beach is possible by stairs.

One of the most important parameters to be studied for coastal problems is the longshore sand transport LST (net and gross values), which requires detailed information of the offshore and nearshore wave climates, preferably based on measured wave data (offshore buoys) in combination with deep water wave modelling. Based on this, semi-empirical LST-equations can be used to compute the annual LST-values along the coast (LONGMOR-model) including the effects of the various influential parameters (sand size, beach slope, wave breaking parameters, coastline orientation). This information is essential for a good understanding of coastal processes and sediment budgets involved^[47]. In addition, detailed cross-shore transport models can be used to better include the effect of the shape of the beach profile on longshore and cross-shore transport processes (CROSMOR-model).

Future research should be focused on the integration of longshore and cross-shore models into a practical coastal model, which can be used for both short-term and long-term

predictions. Observed coastline changes on both sides of short and long groynes (Soulac example; Lagos coast example; recent Rafraf beach example) are essential for proper calibration of these types of coastal models^[48]. Coastal monitoring using modern techniques (drone and satellite imagery) is an essential element in coastal protection and modelling^[49].

Coastal engineers and also policymakers should realise that the design and construction of hard structures is not a straightforward process based on exact science, but rather an iterative process consisting of an initial design based on numerical and physical modelling, the testing of the design by a field pilot project including a monitoring program and the fine tuning of the design by modification of length, spacing and crest levels. It is most cost-effective to design relatively short groynes at wide spacing in the initial phase. If necessary, short groynes can later be extended in seaward direction and/or additional groynes can be placed to reduce the spacing. Straight groynes can also be extended to construct L-head and T-head groynes to improve the trapping of sand in the groyne compartments. More modelling studies should be done to determine the optimum dimensions of these latter types of groynes for trapping of sand. This type of “learning by doing” approach requires sufficient financial means over longer periods of time anchored in a detailed coastal master plan made by the policymakers involved.

Finally, it is noted that hard structures (groynes and breakwaters) generally are seen as unattractive, visual elements blocking the view of the tourists, particularly when the rocks are dumped as riprap instead of being orderly placed. The inefficiency of many traditional (open) groin field systems in protecting the coastline, along with much higher social importance nowadays given to environmental, recreational and aesthetic values, has caused a shift in beach developments. Modern landscaping ideas are focused on the design of long and wide beaches with a minimum number of structures enhancing the natural appearance of the beach. Structures should be designed and planned as multifunctional facilities. Some countries (Spain, Italy) around the Mediterranean have launched initiatives to adopt a new coastal policy of replacing the traditional small-scale groin fields by large-scale recreational beaches^[4]. This policy basically consists of the removal of ineffective and non-aesthetical coastal groins in combination with new beach fill operations, while keeping the terminal groins combined with a submerged or

low-crested breakwater in the middle of the beach to give sufficient protection against wave attack. Such a design might offer a much better aesthetic solution at many places. This may also improve bathing safety as the larger waves will break on the low-crested, detached breakwater in the middle of the beach. Wave diffraction around the terminal groins will promote shoreline curvature towards both ends of the beach, creating a visually, attractive crescent bay-type beach. Beach restoration requires close collaboration between policymakers, coastal engineers and landscape architects to arrive at an attractive, sustainable coastal beach protection scheme in harmony with its surroundings. This is the way forward in better coastal development.

Funding

This research received no external funding.

Institutional Review Board Statement

Not applicable.

Informed Consent Statement

Not applicable.

Data Availability Statement

At request, data used in this study are available for other researchers.

Conflict of interest

The author declares no conflict of interest.

References

- [1] van Rijn, L.C., 2006. Principles of sedimentation and erosion engineering in rivers, estuaries and coastal seas. Aqua Publications: Amsterdam, The Netherlands.
- [2] van Rijn, L.C., 2010. Coastal erosion control based on the concept of sediment cells. Conscience Project, Deltares: Delft, The Netherlands.
- [3] van Rijn, L.C., 2011b. Coastal erosion and control. *Ocean & Coastal Management*. 54(12), 867–887. DOI: <https://doi.org/10.1016/j.ocecoaman.2011.05.004>
- [4] Fleming, C.A., 1990. Guides on the uses of groynes in coastal engineering. CIRIA: London, UK. pp. 1–50.
- [5] Kraus, N.C., Hanson, H., Blomgren, S.H., 1994. Modern functional design of groin systems. Proceedings of the 24th International Conference on Coastal Engineering; 23–28 October 1994; Kobe, Japan. pp. 1327–1342.
- [6] US Army Corps of Engineers, 1994. Coastal groins and nearshore breakwaters. Technical Engineering and Design Guide No. 6. ASCE: Reston, VA, USA.
- [7] van Rijn, L.C., 1998. Principles of Coastal Morphology. Aqua Publications: Amsterdam, The Netherlands.
- [8] Ranasinghe, R., Turner, I.L., 2006. Shoreline response to submerged structures: a review. *Coastal Engineering*. 53(1), 65–79. DOI: <https://doi.org/10.1016/j.coastaleng.2005.08.003>
- [9] El-Sharnouby, B., Soliman, A., 2011. Behavior of shore protection structures at Alexandria, Egypt during the storm of December 2010. Proceedings of the 2011 Conference on Coastal Engineering Practice; 21–24 August 2011; San Diego, California, USA. pp. 780–792.
- [10] Gómez-Pina, G., 2004. The importance of aesthetic aspects in the design of coastal groins. *Journal of Coastal Research*. SI33, 83–98.
- [11] Hulsbergen, C.H., Bakker, W.T., Van Bochove, G., 1976. Experimental verification of groyne theory. Proceedings of the 15th International Conference on Coastal Engineering; 11–17 July 1976; Honolulu, HI, USA. Publication No. 176, Deltares/Delft Hydraulics: Delft, The Netherlands.
- [12] Eslami Arab, S., 2009. A numerical study on design of normal and T-head groynes [MSc Thesis]. Delft, The Netherlands: Delft University of Technology.
- [13] Kana, T.W., White, T.E., McKee, P.A., 2004. Management and engineering guidelines from groin rehabilitation. *Journal of Coastal Research*. SI33, 57–82.
- [14] Shabica, C., 2004. Evolution and performance of groynes on a sediment-starved coast; the Illinois shore of Lake Michigan, North of Chicago, 1880–2000. *Journal of Coastal Research*. SI33, 39–56.
- [15] Basco, D.R., Pope, J., 2004. Groyne functional design guidance from the Coastal Engineering Manual. *Journal of Coastal Research*. SI33, 121–130.
- [16] Soliman, A., El-Sharnouby, B., El-Kamhaway, H., 2014. Shoreline changes due to construction of Alexandria submerged breakwaters, Egypt. Proceedings of the International Conference of Hydrosience and Engineering; 28 September–2 October 2014; Hamburg, Germany. pp. 675–684.
- [17] van Rijn, L.C., 2014. A simple general expression for longshore transport of sand, gravel and shingle. *Coastal Engineering*. 90, 23–39. DOI: <https://doi.org/10.1016/j.coastaleng.2014.04.008>
- [18] Tonnon, P.K., Huisman, B.J.A., Stam, G.N., et al., 2018. Numerical modelling of erosion rates, life span and maintenance volumes of mega nourishments. *Coastal Engineering*. 131, 51–69. DOI:

- <https://doi.org/10.1016/j.coastaleng.2017.10.001>
- [19] van Rijn, L.C., Wijnberg, K.M., 1996. One-dimensional modelling of individual waves and wave-induced longshore currents in the surf zone. *Coastal Engineering*. 28(1–4), 121–145. DOI: [https://doi.org/10.1016/0378-3839\(96\)00014-2](https://doi.org/10.1016/0378-3839(96)00014-2)
- [20] van Rijn, L.C., Walstra, D.J.R., Grasmeijer, B., et al., 2003. The predictability of cross-shore bed evolution of sandy beaches at the time scale of storms and seasons using process-based profile models. *Coastal Engineering*. 47, 295–327. DOI: [https://doi.org/10.1016/S0378-3839\(02\)00120-5](https://doi.org/10.1016/S0378-3839(02)00120-5)
- [21] van Rijn, L.C., 2011a. Principles of fluid flow and surface waves in rivers, estuaries and coastal seas. Aqua Publications: Amsterdam, The Netherlands.
- [22] Isobe, M., Horikawa, K., 1982. Study on water particle velocities of shoaling and breaking waves. *Coastal Engineering in Japan*. 25(1), 109–123. DOI: <https://doi.org/10.1080/05785634.1982.11924340>
- [23] van Rijn, L.C., 1993. Principles of sediment transport in rivers, estuaries and coastal seas. Aqua Publications: Amsterdam, The Netherlands.
- [24] van Rijn, L.C., 2007a. Unified view of sediment transport by currents and waves, I: Initiation of motion, bed roughness and bed-load transport. *Journal of Hydraulic Engineering*. 133(6), 649–667. DOI: [https://doi.org/10.1061/\(ASCE\)0733-9429\(2007\)133:6\(649\)](https://doi.org/10.1061/(ASCE)0733-9429(2007)133:6(649))
- [25] van Rijn, L.C., 2007b. Unified view of sediment transport by currents and waves, II: Suspended transport. *Journal of Hydraulic Engineering*. 133(6), 668–689. DOI: [https://doi.org/10.1061/\(ASCE\)0733-9429\(2007\)133:6\(668\)](https://doi.org/10.1061/(ASCE)0733-9429(2007)133:6(668))
- [26] van Rijn, L.C., 2007c. Unified view of sediment transport by currents and waves, III: Graded beds. *Journal of Hydraulic Engineering*. 133(7), 761–775. DOI: [https://doi.org/10.1061/\(ASCE\)0733-9429\(2007\)133:7\(761\)](https://doi.org/10.1061/(ASCE)0733-9429(2007)133:7(761))
- [27] Putnam, J.A., Arthur, R.S., 1948. Diffraction of water waves by breakwaters. *EOS Transactions American Geophysical Union*. 29(4), 455–606. DOI: <https://doi.org/10.1029/TR029i004p00481>
- [28] Briggs, M.J., Thompson, E.F., Vincent, C.L., 1995. Wave diffraction around breakwater. *Journal of Waterway, Port, Coastal, and Ocean Engineering*. 121(1), 23–35. DOI: [https://doi.org/10.1061/\(ASCE\)0733-950X\(1995\)121:1\(23\)](https://doi.org/10.1061/(ASCE)0733-950X(1995)121:1(23))
- [29] Goda, Y., 1985. Random seas and design of maritime structures. University of Tokyo Press: Tokyo, Japan.
- [30] Goda, Y., Takayama, T., Suzuki, Y., 1978. Diffraction diagrams for directional random waves. *Proceedings of the 16th International Conference on Coastal Engineering*; 27 August–3 September 1978; Hamburg, Germany. pp. 628–650. DOI: <https://doi.org/10.1061/9780872621909.037>
- [31] Illic, S., Van der Westhuysen, A.J., Roelvink, J.A., et al., 2007. Multidirectional wave transformation around detached breakwaters. *Coastal Engineering*. 54, 775–789. DOI: <https://doi.org/10.1016/j.coastaleng.2007.05.002>
- [32] Kamphuis, J.W., 1992. Short course on design and reliability of coastal structures. Chapter 9. *Proceedings of the 23rd International Conference on Coastal Engineering*; 4–9 October 1992; Venice, Italy.
- [33] Aubie, S., Tastet, J.P., 2000. Coastal erosion, processes and rates: an historical study of the Gironde coastline, southwestern France. *Journal of Coastal Research*. 16(3), 756–767.
- [34] Lerma, A.N., Ayache, B., Ulvoas, B., et al., 2019. Pluriannual beach-dune evolutions at regional scale: Erosion and recovery sequences analysis along the Aquitaine coast based on airborne LiDAR data. *Continental Shelf Research*. 189, 103974. DOI: <https://doi.org/10.1016/j.csr.2019.103974>
- [35] Casagec, 2020. Study of coastal protection near Soulac-sur-mer, France (in French). *Rapport CI-19055-A*, Anglet, France.
- [36] Idier, D., Castelle, B., Charles, E., et al., 2013. Long-shore sediment flux hindcast: spatio-temporal variability along the SW Atlantic coast of France. *Journal of Coastal Research*. 65(sp2), 1785–1790. DOI: <https://doi.org/10.2112/SI65-302.1>
- [37] EIA, 2012. Environmental Impact Assessment Eko Atlantic City project. Lagos, Nigeria.
- [38] Nwilo, P.C., 1995. Sea level variations and the impacts along the Nigerian coastal areas [PhD Thesis]. Salford, UK: University of Salford.
- [39] Nwilo, P.C., 1997. Managing the impacts of storm surges on Victoria island, Lagos, Nigeria. *Proceedings of the Conference on Destructive Water*; June 1996; Anaheim, CA, USA. IAHS Publication No. 239.
- [40] Olaniyou, E., Afiesimama, E.A., 2004. Understanding Ocean surges. Marine and Oceanography Laboratory, Nigeria Meteorological Agency: Lagos, Nigeria.
- [41] Folorunsho, R., Salami, M., Ayinde, A., et al., 2023. The salient issues of coastal hazards and disasters in Nigeria. *Journal of Environmental Protection*. 14(5), 1–15. DOI: <https://doi.org/10.4236/jep.2023.145021>
- [42] Awosika, L., 2015. Assessment of morphological changes to the Kuramo Waters and adjoining Mondinvest property resulting from the dredging activities for the EKO Atlantic City project Lagos. Department Marine Geology/Geophysics, Nigerian Institute for Oceanography and Marine Research: Lagos, Nigeria.
- [43] Van Bentum, K.M., 2012. The Lagos Coast; investigation of the long-term morphological impact of the EKO Atlantic City project [MSc Thesis]. Delft, The Netherlands: Delft University of Technology.
- [44] Bijl, E., Van der Spek, B.J., Heijboer, D., 2022. Hydraulic performance of low-crested breakwaters protecting a beach nourishment in an energetic swell wave climate. *CDR International*: Amersfoort, The Netherlands.

- lands.
- [45] Stockdon, H.F., Holman, R.A., Howd, P.A., et al., 2006. Empirical parameterization of setup, swash and runup. *Coastal Engineering*. 53, 573–588.
- [46] van Rijn, L.C., Mol, A., Kroeders, M., 2025. Design of Artificial Beaches at Sheltered and Exposed Sites. *Journal of Environmental and Earth Science*. 7(1), 588–610. DOI: <https://doi.org/10.30564/jees.v7i1.7444>
- [47] van Rijn, L.C., Geleynse, N., Perk, L., et al., 2025. Longshore sediment transport and sediment budgets, South-East Florida coast, USA. *Journal of Coastal Research*. DOI: <https://doi.org/10.2112/jcoastres-d-24-00070.1>
- [48] Saidi, H., Guebsi, R., Chaabani, C., et al., 2024. Assessment of coastal changes following the construction of a groyne using satellite and drone imagery along the Mediterranean coast of North-West Tunisia (Rafraf, Bizerte). *Euro-Mediterranean Journal for Environmental Integration*. 9, 1009–1020. DOI: <https://doi.org/10.1007/s41207-023-00456-1>
- [49] Abd-Elhamid, H.F., Abdelfattah, M., Zelenakova, M., et al., 2025. Monitoring coastal changes in Port Said, Egypt using multi-temporal satellite imagery and GIS-DSAS. *Modelling Earth Systems and Environment*. 11, 56. DOI: <https://doi.org/10.1007/s40808-024-02266-y>